Chapter 3

Reproducibility of Wall Shear Stress Assessment with the Paraboloid Method in the Internal Carotid Artery with Velocity Encoded MRI in Healthy Young Individuals

Frieke MA Box, Rob J van der Geest, Jeroen van der Grond, Matthias JP van Osch, Aeilko H Zwinderman, Inge H Palm-Meinders, Joost Doornbos, Gerard J Blauw, Mark A van Buchem, Johan HC Reiber

From the Division of Image Processing (F.M.A.B., R.J.vd G., J.H.C.R.) of the Department of Radiology (J.vd.G., M.J.P.v O., I.H.P.M., M.A.v B.), and from the Departments of Gerontology & Geriatrics (G.J.B.) Leiden University Medical Center, Leiden, and the Dept Clin Epidemiol & Biostat (A.H.Z.), Acad Med Ctr, Univ Amsterdam, the Netherlands

JMRI, in press

Abstract

Purpose: To verify whether Wall Shear Stress (WSS) can be assessed in a reproducible manner, using automatic model-based segmentation of phase-contrast MR images, by determination of flow volume and maximum flow velocity (Vmax) in cross-sections of these vessels.
Materials and Methods: The approach is based on fitting a 3D paraboloid to the actual velocity profiles and on determining Vmax. WSS was measured in the internal carotid arteries of two groups of healthy young volunteers. Reproducibility of rescanning and repositioning was studied in the first group. In the second group a one-week and a one-month interval was investigated. Reproducibility was calculated by the intraclass correlation (ICC).
Results: The flow volume, Vmax and WSS averaged over the cardiac cycle were found to be 287.8 ± 29.7 ml/min, 37.0 ± 4.6 cm/s and 1.13 ± 0.16 Pa respectively. The diastolic WSS varied between 1.00 ± 0.21 Pa without averaging tot 0.88 ± 0.16 Pa with temporal and spatial averaging. Systolic WSS was 1.67 ± 0.33 Pa without averaging and 1.67 ± 0.25 Pa with averaging. ICC varied between 0.58 and 0.87 without averaging and between 0.75 and 0.90 with averaging for WSS.
Conclusion: WSS in MR images of the internal carotid artery can be assessed semi-automatically with a good to excellent reproducibility without inter- or intra observer variability using model-based post-processing.

3.1 Introduction

It is well known that a correlation exists between the presence of atherosclerosis and arterial Wall Shear Stress (WSS) (1). WSS is defined as the mechanical frictional force exerted on the vessel wall by flowing blood. WSS (Pa) is defined by the wall shear rate γ (s^{-1}) multiplied by the dynamic viscosity η (Pa.s). Under the assumption of a parabolic velocity profile, WSS can be calculated for medium sized vessels such as the common and internal carotid arteries by means of MRI and ultrasound. For a parabolic velocity profile, there is a fixed relation between the three parameters diameter, flow and Vmax. When two out of the three parameters can be determined accurately, it is assumed that WSS can be assessed with a high accuracy and precision (2,3). It was demonstrated, that individual flow volume and velocity measurements can be performed non-invasively by phase-contrast MR flow velocity mapping, by assessing velocity profiles in vessels for different phases of the cardiac cycle (4,5). An accurate diameter determination of medium sized vessels, such as the internal carotid artery, is difficult, because of the low image resolution. Therefore, the other two parameters, being the flow volume and the maximum velocity in the cross sectional images (Vmax) are crucial when assessing the WSS accurately and reproducibly.
The assumption of a parabolic velocity profile is valid for small vessels to medium sized vessels (6) and is widely used for the WSS determination by ultrasound and MRI in the carotid and similarly sized arteries (2,7,8,910,11). Flow volume and Vmax can both be assessed during different stages (phases) of the cardiac cycle. Therefore we were capable to assess the WSS averaged over the cardiac cycle (MWSS), during diastole (DWSS) and during systole (SWSS). All these parameters can be assessed without inter- or intra observer variability after one click of the mouse, within the vessel of interest (12). For diagnostic purposes and for applications in clinical-trails, it is essential to have a high reproducibility so that the effect of treatment on the WSS can be assessed with sufficient accuracy (13,14). The goal of this work was to assess the accuracy and reproducibility of this WSS approach using a population of volunteers.

3.2 Materials and Methods

3.2.1 Study design

A method to assess the WSS in the internal carotid artery in a reproducible and rapid manner that only needs user-interaction for initialisation was developed and tested. The method is based on a first approximation of blood flow properties, which is a parabolic velocity profile (Fig. 1) (2). The blood flow volume, Vmax and WSS were assessed in the internal carotid arteries in 27 healthy volunteers. A first group of 7 young volunteers (4 males, age 24.9 ± 3.5 years) was scanned three times.
To assess the stability of WSS measurements (rescanning) on a given MR system, a second scan was performed directly after the first one, while the volunteer remained inside the MR scanner. To assess the influence of repositioning a patient in the MR system, which may give rise to variation in location and angle of the flow measurement, a third acquisition procedure was performed after the volunteer left the MR scanner and was repositioned. For the third scan, new surveys were acquired and the flow measurement was planned on these new surveys. The second group consisted of 20 young volunteers, (10 males, age 27.4 ± 6.7 years) and was scanned three times. The first follow-up was after one week, and the second follow-up after 3 to 4 weeks after the initial scan.

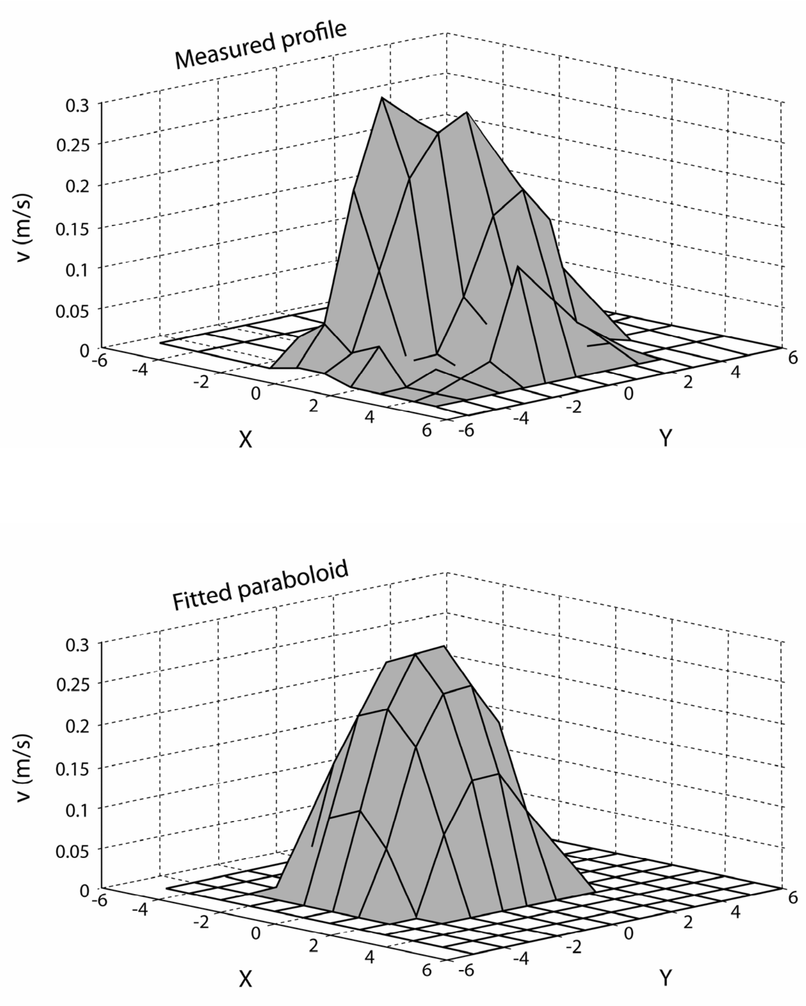

Figure 1. An example of a paraboloid (below) that was fitted to an actual velocity profile (above).

3.2.2 Acquisition procedures

To measure velocity profiles in the internal carotid arteries MR examinations were performed on a 1.5 T clinical MR system (Gyroscan NT; Philips Medical Systems, Best, the Netherlands) using a standard head coil. Measurements were performed 4 to 5 cm above the carotid bifurcation. In the group of 7 volunteers retrospective cardiac gating was performed by means of a peripheral pulse unit. In the second group of 20 volunteers a vector ECG was used. In both groups 16 scans (phases) were acquired over the cardiac cycle. The imaging parameters in both groups were: Echo Time (TE) 9 ms, Repetition Time (TR) 16 ms, 7.5° flip angle, 5 mm slice thickness, 250 × 188 mm field of view, scan matrix 256 × 154 and a velocity sensitivity of 100 cm/s in the feet-head direction. The number of signal averages was 1; the acquired voxel size was 0.98/ 1.22/ 5.00 mm and the reconstructed voxel size was 0.98/ 0.98/ 5.00 mm. Read-out bandwidth was 48 kHz. Flow encoding was interleaved every TR. The scan time was dependent on the heart rate, being approximately 3 minutes at 60 beats/min.

3.2.3 Quantitative analysis approach

Quantification of WSS from such MR examinations requires a post-processing step to differentiate the voxels within a vessel's cross-section from the surrounding background tissue. To segment the region-of-interest (ROI) automatically and as accurately as possible, the average velocity profile over the complete cardiac cycle is fitted to a parabolic velocity profile. The ROI consists out of those voxels where the fitted parabolic profile has a positive value. The individual blood flow volumes are calculated by the multiplication of the actual velocity values and the area of the ROI. Inside the ROI, the voxel with the highest velocity (Vmax) is selected for each time slice. During a velocity-encoded MR study, phase difference and standard modulus images are acquired at multiple time points in the cardiac cycle. Since phase images show good contrast, even in the absence of flow, the analysis algorithm was developed to operate on phase images. The method does not require manual interaction. The basic steps in the quantitative analysis of the velocity encoded cine MR imaging studies was carried out with the analytical software package MRI-FLOW; details were described elsewhere (16). In brief: MRI-FLOW gives the velocity profiles in cross sectional images and allows addition of contours from which flow volume and velocities can be assessed.

3.2.4 Automatic flow volume, diameter and WSS assessment for small vessels

To assess the WSS in the internal carotid artery, we have assumed the cross section of the vessel to be circular and the velocity profile to be parabolic. This parabolic velocity profile is fitted on the phase image, after initialising the procedure with a mouse click in the vessel of interest. The fitting procedure with the results for automatic flow estimation is described in detail elsewhere (12). In brief, it is based on the following principles: an average velocity image was derived from all data collected over the cardiac cycle. The average velocity profile was thresholded at the level of 0.43 times the Vmax of the average profile. Voxels with velocities below this threshold were rejected, and the paraboloid was fitted on the remaining data. The voxels for which the fitted parabolic velocity profile had positive flow volumes, were assumed to be inside the vessel. After that the average flow velocity was calculated by averaging the velocity values from the individual pixels in the segmented area for each phase in the cardiac cycle. Diastolic flow was assessed by taking the phase in the cardiac cycle before systole. Systolic flow was assessed by taking the phase in the cardiac cycle with the highest flow volume. The WSS can be calculated as follows (3):

$$\mathrm{WSS} = 4\mu \mathrm{Vmax}/D \qquad (1)$$

where Vmax is the maximum velocity in the cross section and μ being the blood viscosity. Blood is assumed to be a Newtonian fluid and the viscosity is taken as 4.6 mPas (3). The diameter D of the vessel was calculated from the flow data using the Hagen-Poiseuille formula (2):

$$D = \mathrm{sqrt}(8Q/\mathrm{Vmax}\ \pi) \qquad (2)$$

where Q is the flow volume in m^3/s. Combining Eq 1 and Eq 2 yields:

$$\text{WSS} = \mu \text{ Vmax sqrt}(2\pi\text{Vmax}/Q) \quad (3)$$

It has been shown that Q can be assessed with an excellent reproducibility by MRI (12). Vmax is the most reliable assessable velocity parameter with MRI. Vmax has least noise and minimal partial volume effects compared to other velocities, which can be measured with MRI (17). Therefore Eq. 3 was used to calculate the WSS. A quality parameter was used to examine the difference between the fitted paraboloid and the actual velocity profile. This quality parameter was defined as the sum of squared differences between the fitted values and the measurement values divided by the number of voxels inside the segmented area. The fittings were designated 'inadequate' when the difference between the measurements and the fitting was above a certain threshold. The fit quality was defined as:

$$\text{Fit quality}=\Sigma^{ROI} \text{sqrt}(\text{measured velocity}_i\text{-u}(x_i,y_i))^2 , \quad (4)$$

where ROI is the region of interest being the segmented area. The threshold was 0.63 cm/s, which means that for 15 voxels the average difference between fit and measurement had to stay below 0.04 cm/s per voxel. When the fit was characterized as 'inadequate' the scan was excluded (12). In this study the cardiac cycle was divided into 16 time slices (phases).

3.2.5 Statistical analysis

To assess the reproducibility of data in the young individuals, the coefficient of variation (CV) and the Intra Class Correlation (ICC) were calculated. The CV was defined as SD_{REP}/mean where SD_{REP} was determined by taking the standard deviation of all the signed differences of corresponding repeated measurements (18). Thus if diff_i=measurement1_i-mesurement2_i then SD_{REP} = the standard deviation of diff. The ICC is defined as: $(S_T^2 / (S_T^2 + S_e^2))$, were $S^2{}_T$ is the component of variance due to error free variability among subjects and S_e^2 is the component of variance due to the random measurement error (19). Also the 95% confidence interval (95% CI) of the ICC was determined. SPSS was applied to calculate the ICC.

The reproducibility was tested for the flow volume, Vmax , diameter and the WSS data averaged over the cardiac cycle FlowM, VmaxM, DiamM, MWSS), the diastolic phases of the cardiac cycle (FlowD, VmaxD, DiamD, DWSS), as well as during peak systole (FlowS, VmaxS, DiamS, SWSS). For these parameters the standard deviations, CV and ICC were determined for rescanning, repositioning, baseline to the first follow-up after one week, and for baseline to the second follow-up after one month. To decrease noise and increase reproducibility, the diastolic phases and systolic phases were averaged over three phases. This is indicated by the postfix 3t. Aiming at even more increase in reproducibility the tests were repeated for averaging over the 4 voxels with the highest Vmax, the results were indicated by the postfix 4. In case both temporal and spatial averaging were used, this was indicated by the postfix 3t4.

The Bland-Altman method was applied to illustrate the differences and the standard deviations of repeated measurements (20). For a Bland-Altman analysis the difference of two repeated measurements is shown on the y-axis and the average on the x-axis. Two times the standard deviation of the difference ($2*SD_{REP}(d)$) is indicated in the graph.

	Rescanning (N=14)			Repositioning (N=13)		
	Mean ± SD_{REP}	**CV (%)**	**ICC (95% CI)**	**Mean ± SD_{REP}**	**CV (%)**	**ICC (95% CI)**
FlowM	273.8 ± 18.1	6.6	0.95 (0.85-0.98)	267.2 ± 15.1	5.7	0.96 (0.87-0.99)
FlowD	208.5 ± 25.0	12.0	0.85 (0.60-0.95)	202.3 ± 16.1	8.0	0.92 (0.76-0.98)
FlowS	409.4 ± 28.9	7.1	0.97 (0.91-0.99)	401.2 ± 45.0	11.2	0.91 (0.73-0.97)
VmaxM	37.9± 3.2	8.4	0.90 (0.73-0.97)	37.9 ± 3.3	8.7	0.88 (0.65-0.96)
VmaxD	30.0 ± 4.6	15.3	0.76 (0.40-0.92)	30.5 ± 4.1	13.4	0.68 (0.23-0.89)
VmaxS	54.3 ± 4.4	8.1	0.91 (0.75-0.97)	55.8 ± 7.1	12.7	0.85 (0.59-0.95)
DiamM	5.55 ±0.26	4.7	0.93 (0.79-0.98)	5.46 ±0.27	4.9	0.87 (0.63-0.96)
DiamD	5.46 ± 0.42	7.7	0.84 (0.57-0.95)	5.31 ± 0.37	7.0	0.75 (0.37-0.92)
DiamS	5.66 ± 0.40	7.1	0.85 (0.59-0.95)	5.5 ± 0.33	6.0	0.80 (0.47-0.93)
MWSS	1.29 ± 0.16	12.3	0.89 (0.68-0.96)	1.33 ± 0.18	13.7	0.82 (0.51-0.94)
DWSS	1.04 ± 0.24	23.1	0.71 (0.32-0.90)	1.08 ± 0.24	22.2	0.58 (0.07-0.85)
SWSS	1.73 ± 0.21	12.1	0.87 (0.65-0.96)	1.81 ± 0.30	16.6	0.77 (0.38-0.92)
FlowD3t	201.0 ± 18.9	9.4	0.89 (0.69-0.96)	195.8 ± 14.5	7.4	0.93 (0.78-0.98)
FlowS3t	374.7 ± 21.8	5.8	0.97 (0.90-0.99)	363.3 ± 24.0	6.6	0.96 (0.86-0.99)
VmaxD3t	29.6 ± 3.3	11.1	0.89 (0.70-0.96)	29.5 ± 3.9	10.2	0.74 (0.35-0.92)
VmaxD3t	29.6 ± 3.3	11.1	0.89 (0.70-0.96)	29.5 ± 3.9	10.2	0.74 (0.35-0.92)
VmaxS3t	50.4 ± 4.6	9.1	0.86 (0.61-0.95)	50.1 ± 4.9	9.8	0.86 (0.61-0.96)
DiamD3t	5.41 ± 0.31	5.7	0.91 (0.74-0.97)	5.33 ± 0.33	6.2	0.82 (0.52-0.94)
DiamS3t	5.63 ± 0.35	6.2	0.86 (0.61-0.95)	5.56 ± 0.33	5.9	0.82 (0.52-0.94)
DWSS3t	1.09 ± 0.21	19.2	0.83 (0.54-0.94)	1.12 ± 0.19	16.	0.77 (0.40-0.92)
SWSS3t	1.68 ± 0.23	13.9	0.85 (0.59-0.95)	1.72 ± 0.26	14.9	0.79 (0.45-0.93)
VmaxM4	34.6± 2.8	8.0	0.91 (0.74-0.97)	34.6 ± 2.8	8.0	0.89 (0.68-0.97)
VmaxD3t4	26.8 ± 2.5	9.3	0.89 (0.68-0.96)	26.6 ± 2.8	10.5	0.81 (0.50-0.94)
VmaxS3t4	46.2± 3.5	7.6	0.93 (0.80-0.98)	46.0 ± 4.7	10.2	0.86 (0.61-0.96)
DiamM4	5.79 ± 0.26	4.4	0.92 (0.78-0.97)	5.45 ± 0.25	4.6	0.89 (0.65-0.96)
DiamD3t4	5.67 ± 0.31	4.6	0.90 (0.71-0.97)	5.59 ± 0.32	5.7	0.79(0.44-0.93)
DiamS3t4	5.88 ± 0.30	5.1	0.89 (0.70-0.96)	5.80 ± 0.31	5.3	0.81(0.50-0.94)
MWSS4	1.12 ± 0.13	11.9	0.87 (0.65-0.96)	1.15 ± 0.14	12.0	0.83 (0.54-0.95)
DWSS3t4	0.94 ± 0.16	16.9	0.85 (0.60-0.95)	0.96 ± 0.14	14.4	0.77 (0.40-0.92)
SWSS3t4	1.47 ± 0.18	11.8	0.88 (0.66-0.96)	1.50 ± 0.22	14.9	0.79 (0.44-0.93)

Table 1. The flow volume (ml/min), the maximum velocity (Vmax) in the cross section (cm/s), the diameter (Diam) (mm) and the WSS (Pa) with ± the SD_{REP}, the coefficient of variation (CV) (%) and the Intra Class correlation (ICC) with in between brackets the 95% reliability intervals. The letters M, S and D refer to mean values over the cardiac cycle, those at end-systole and end-diastole, respectively. The postfix 3t indicates an averaging over 3 phases in the cardiac cycle. The postfix 4 indicates an averaging over the four central voxels

3.3 Results

3.3.1 Reproducibility for flow volume, diameter and WSS in individual vessels

The short-term reproducibility was tested in 7 volunteers who were scanned 3 times within a 1 hour period. The results for rescanning and repositioning are shown in Table 1. The data for the repositioning analyses showed one large outlier, which was caused by a vessel where the scan plane in the first scan was not perpendicular to the vessel. This outlier was removed. The flow volume measurements for both rescanning and repositioning gave an excellent reproducibility with a small CV. For rescanning the mean (=without averaging + 3t + 3t4) ICC for all parameters was 0.95 and the mean CV was 6.6 %; for repositioning it was 0.96 and 5.7 %. For VmaxM, DiamM and MWSS the rescanning gave slightly better results than repositioning. For the VmaxM it was 0.90 with 8.4 % for rescanning and 0.88 with 8.7 % for repositioning. For the DiamM it was 0.93 with 4.7 % for rescanning and 0.87 with 4.9 % for repositioning. For the MWSS it was 0.89 with 12.3 % for rescanning and 0.82 with 13.7 % for repositioning. When the parameters were determined by averaging the four central voxels (indicated by the postfix 4) the results were: For VmaxM4 it was 0.91 with 8.0 % and 0.89 with 8.0 % for rescanning and repositioning respectively. For DiamM4 it was 0.92 with 4.4 % and 0.89 with 4.6 %. For MWSS4 it was 0.87 with 11.9 % and 0.83 with 12.0 %.

In figure 2 the Bland-Altman method was used to present the measurements for repositioning. The thick lines indicate $2*SD_{REP}$ (d) for the results for MWSS4, The thin lines indicate $2*SD_{REP}$ (d) for MWSS. The standard deviations are smaller for MWSS4.

Secondly the long term reproducibility was tested in 20 young volunteers (10 males), average age 26.7 ± 7.1 years. The first follow-up was measured after one week and the second follow-up after 1 month. Measurements without follow-up were excluded from the analysis. The flow volume, Vmax and WSS with CV and ICC are presented in Table 2. At baseline one scan could not be used due to data conversion errors. During the first follow-up 4 scans had data conversion errors, therefore, 30 individual vessels were used for the analysis. In the second follow-up one scan had errors, leaving 36 individual vessels available for statistical analysis. No scans were excluded because of insufficient fit-quality. The CV and ICC for the WSS were generally smaller for one-week follow-up compared to the second follow-up after one month.

Reproducibility was best for rescanning, followed by follow–up after one week, after that repositioning and the follow-up after one month gave the smallest ICC. The ICC for the WSS4 was on average 0.87, 0.80, 0.86 and 0.77 respectively. In figure 3 the Bland-Altman method was used to present the measurements for repositioning. The thick lines indicate $2*SD_{REP}$ (d) for the results for MWSS4; the thin lines indicate $2*SD_{REP}$ (d) for MWSS. The standard deviations are smaller for WSS4.

	Baseline – 1 week follow up (N=30)			Baseline – 1 month follow up (N=36)		
	Mean ± SD_{REP}	**CV (%)**	**ICC (95% CI)**	**Mean ± SD_{REP}**	**CV (%)**	**ICC (95% CI)**
FlowM	297.2 ± 31.2	10.5	0.82 (0.65-0.91)	286.7 ± 30.4	10.6	0.86 (0.75-0.93)
FlowD	196.9 ± 44.6	22.7	0.53 (0.23-0.74)	189.1 ± 47.8	25.3	0.49 (0.19-0.70)
FlowS	479.3 ± 76.1	15.9	0.73 (0.51-0.86)	462.1 ± 69.1	15.0	0.81 (0.65-0.90)
VmaxM	36.1 ± 3.6	10.0	0.84 (0.69-0.92)	36.0 ± 5.2	14.4	0.61 (0.35-0.78)
VmaxD	28.6 ± 5.1	17.8	0.43 (0.10-0.67)	27.8 ± 6.7	24.1	0.20 (-0.13-0.49)
VmaxS	52.6 ± 7.7	14.6	0.78 (0.60-0.89)	53.1 ± 9.1	17.1	0.65 (0.42-0.81)
DiamM	6.14 ± 0.35	5.7	0.84 (0.68-0.92)	6.03 ± 0.33	5.5	0.86 (0.74-0.92)
DiamD	5.81 ± 0.63	10.8	0.59 (0.31-0.78)	5.69 ± 0.69	12.1	0.52 (0.23-0.72)
DiamS	6.44 ± 0.46	7.1	0.77 (0.57-0.88)	6.27 ± 0.41	6.5	0.79 (0.63-0.89)
MWSS	1.15 ± 0.15	13.1	0.89 (0.78-0.95)	1.17 ± 0.20	17.4	0.76 (0.57-0.87)
DWSS	0.95 ± 0.22	22.8	0.64 (0.38-0.81)	0.98 ± 0.19	18.8	0.72 (0.51-0.85)
SWSS	1.58 ± 0.28	17.5	0.82 (0.66-0.91)	1.64 ± 0.36	21.9	0.71 (0.50-0.84)
FlowD3t	211.3 ± 26.8	12.7	0.79 (0.61-0.89)	203.6 ± 32.3	15.9	0.76 (0.58-0.87)
FlowS3t	427.3 ± 54.0	12.6	0.77 (0.57-0.88)	410.7 ± 41.6	10.1	0.87 (0.77-0.93)
VmaxD3t	28.7 ± 3.3	11.5	0.81 (0.64-0.90)	28.8 ± 4.3	14.9	0.63 (0.38-0.79)
VmaxS3t	48.2 ± 4.8	10.0	0.83 (0.68-0.92)	48.1 ± 7.4	15.4	0.61 (0.36-0.78)
DiamD3t	5.88 ± 0.40	6.8	0.76 (0.55-0.88)	5.78 ± 0.43	7.4	0.77 (0.59-0.88)
DiamS3t	6.35 ± 0.43	6.8	0.76 (0.56-0.88)	6.22 ± 0.34	5.5	0.84 (0.72-0.92)
DWSS3t	0.97 ± 0.16	16.7	0.82 (0.66-0.91)	0.99 ± 0.18	17.4	0.77 (0.59-0.87)
SWSS3t	1.47 ± 0.18	12.3	0.89 (0.79-0.95)	1.50 ± 0.30	20.0	0.70 (0.49-0.84)
VmaxM4	33.4 ± 3.1	9.3	0.85 (0.72-0.93)	33.2 ± 4.4	13.3	0.61 (0.36-0.78)
VmaxD3t4	25.1 ± 2.9	11.6	0.91 (0.83-0.96)	25.0 ± 3.4	13.6	0.85 (0.73-0.92)
VmaxS3t4	43.0 ± 4.0	9.3	0.96 (0.91-0.98)	43.2 ± 6.1	14.1	0.89 (0.79-0.94)
DiamM4	6.13 ± 0.34	5.5	0.84 (0.68-0.92)	6.02 ± 0.32	5.3	0.86 (0.74-0.92)
DiamD3t4	5.85 ± 0.42	7.2	0.71 (0.48-0.85)	5.75 ± 0.42	7.3	0.75 (0.57-0.87)
DiamS3t4	6.35 ± 0.43	6.8	0.77 (0.56-0.88)	6.22 ± 0.34	5.5	0.84 (0.72-0.92)
MWSS4	1.00 ± 0.12	12.8	0.90 (0.80-0.95)	1.01 ± 0.16	16.0	0.79 (0.63-0.89)
DWSS3t4	0.83 ± 0.13	15.4	0.82 (0.65-0.91)	0.84 ± 0.13	15.4	0.76 (0.58-0.87)
SWSS3t4	1.34 ± 0.19	14.4	0.86 (0.72-0.93)	1.36 ± 0.23	17.3	0.75 (0.56-0.86)

Table 2. The data for the follow-ups after one-week and one-month. The flow volume (ml/min), the maximum velocity (Vmax) in the cross section (cm/s), the diameter (Diam) (mm) and the WSS (Pa) with ± the SD_{REP}, the coefficient of variation (CV) (%) and the Intra Class correlation (ICC) with in between brackets the 95% reliability intervals. The letters M, S and D refer to mean values over the cardiac cycle, those at end-systole and end-diastole, respectively. The postfix 3t indicates an averaging over 3 phases in the cardiac cycle. The postfix 4 indicates an averaging over the four central voxels.

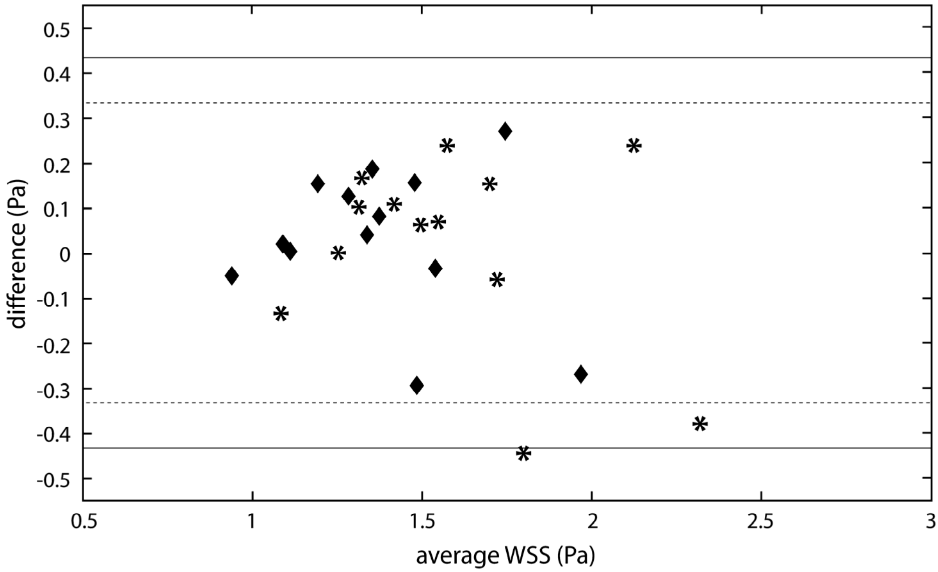

Figure 2. The Bland-Altman plot for repositioning. The lines indicate $2*SD_{REP}$ (d), the full lines are used for MWSS, the dashed lines indicate MWSS4. Individual measurements are indicated with * for MWSS and ♦ for MWSS4.

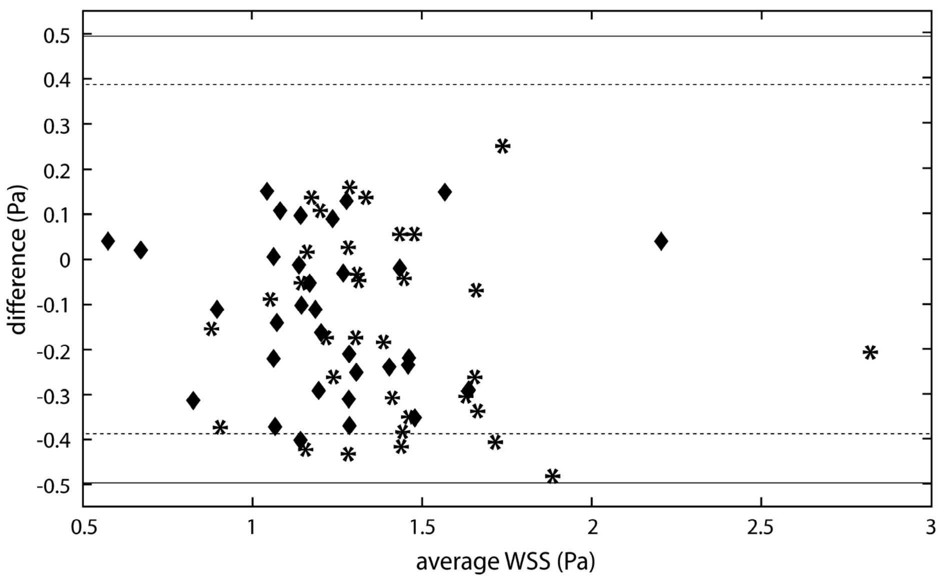

Figure 3. The Bland-Altman plot for follow-up after one month. The lines indicate $2*SD_{REP}$ (d), the full lines are used for MWSS, the dashed lines indicate MWSS4. Individual measurements are indicated with * for MWSS and ♦ for MWSS4.

3.3.2 Effects of resolution decrease for flow volume, diameter and WSS in individual vessels

The effects of resolution decrease by averaging in time (3t), space (4) and time plus space (3t4) are presented in Table 3 and 4. When all single voxel, single phase measurements are averaged FlowM=287.8 ± 29.7 ml/min, VmaxM=37.1 ± 4.6 cm/s and WSSM=1.22 ± 0.19 Pa respectively. DWSS and SWSS were 1.01 ± 0.22 Pa and 1.68 ± 0.34 Pa respectively.
To investigate the influence of averaging over 3 phases in the cardiac cycle and over 4 voxels ICC and CV were calculated for all reproducibility measurements for each parameter. The ICC with the CV for VmaxM based on one voxel and on 4 voxels were: 0.74 with 12.4 % and 0.75 with 11.7 % respectively; for DiamM 0.88 with 6.6 % and for DiamM4 0.86 with 5.3 %; for MWSS 0.82 with 15.6 % and for MWSS4 0.84 with 14.3 %. VmaxM4 is lower than VmaxM, DiamM4 is larger than DiamM and MWSS4 is lower than MWSS. The difference in these parameters was calculated by (parameter-parameter4)/parameter and was 8.1 % for Vmax. The diameter showed an increase and thus the difference was -1.7 %. The decrease of the WSS was 13.9 %.
When all CV's and ICC's were averaged over all parameters the single central voxel, single phase gave an average CV of 15.4 % and an average ICC of 71.4 (0.60-0.80); when the diastolic and systolic phase were averaged over 3 phases (3t) the CV was 12.3 % and the ICC 79.4 (0.71-0.86); if this averaging in time was combined with the averaging over the four central voxels (3t4) the average CV was 11.3% and the ICC was 0.82 (0.75-0.88).

3.4 Discussion

In this study we have investigated the reproducibility of the WSS in the internal carotid artery. Given the size of the arteries supplying the brain, the accuracy is restricted by the image resolution. In a previous article, we proposed a fast, user-independent automatic segmentation approach, which we assume is applicable to the data from any MR-scanner and flow-protocol (12) based on a pragmatic MR TCBF (=total cerebral blood flow) acquisition protocol, yielding accurate and reproducible flow volume data. It was assumed that a parabolic velocity profile is a valid model for the blood flow in the carotid vessels given its small diameter and the relatively constant flow volume over the cardiac cycle. The proposed automatic segmentation approach is based on fitting a three-dimensional parabolic velocity profile to the actual velocity data, thus providing boundary positions for the vessel of interest. For studies aiming at detecting small changes in WSS, accurate and reproducible methods are needed.
The method used in this study needs only initialisation by the user and is therefore called semi-automatic. By one mouse click the user needs only to indicate the vessel of interest. The method has no inter- or intra observer variability associated with it. In this study we tested the reproducibility of automated WSS assessment based on the fit of a parabolic velocity profile. To increase reproducibility three phases during systole and during diastole were averaged. To increase reproducibility even more the four central voxels were averaged. With averaging in time and space (3t4) we found a good to excellent reproducibility (ICC; 95% CI) for rescanning (0.86; 0.60 to 0.95), a good reproducibility for repositioning (0.79; 0.45 to 0.93), an excellent reproducibility for follow-up after one week (0.85; 0.71 to 0.93), and a good reproducibility for follow-up after one month (0.75; 0.56 to 0.86) (21).

	Mean ± SD_{REP}	CV (%)	ICC (95% CI)	Mean ± SD_{REP}	CV (%)	ICC (95% CI)
		FlowD			**FlowS**	
Single	198.0 ± 44.9	22.7	0.68 (0.56-0.78)	454.4 ± 68.4	15.1	0.73 (0.63-0.81)
3t	205.8 ± 29.3	14.2	0.78 (0.68-0.85)	406.2 ± 44.0	10.8	0.86 (0.80-0.91)
		VmaxD			**VmaxS**	
Single	29.0 ± 5.7	19.7	0.45 (0.28-0.60)	54.1 ± 8.8	16.3	0.72 (0.60-0.80)
3t	29.4 ± 4.0	13.6	0.73 (0.62-0.81)	49.4 ± 6.4	13.0	0.74 (0.63-0.82)
3t4	25.8 ± 4.0	15.5	0.86 (0.80-0.91)	44.3 ± 5.2	11.7	0.91 (0.86-0.94)
		DiamD			**DiamS**	
Single	5.6 ± 0.63	11.3	0.63 (0.49-0.74)	6.1 ± 0.45	7.4	0.82 (0.74-0.88)
3t	5.7 ± 0.39	6.8	0.82 (0.74-0.88)	6.1 ± 0.38	6.2	0.85 (0.78-0.90)
3t4	6.0 ± 0.32	5.3	0.77 (0.67-0.84)	6.1 ± 0.37	6.1	0.83 (0.76-0.89)
		DWSS			**SWSS**	
Single	1.01 ± 0.22	21.8	0.56 (0.40-0.68)	1.68 ± 0.34	20.2	0.82 (0.74-0.88)
3t	1.03 ± 0.18	17.5	0.78 (0.69-0.85)	1.57 ± 0.26	16.6	0.79 (0.70-0.85)
3t4	0.88 ± 0.14	15.9	0.79 (0.70-0.85)	1.40 ± 0.22	15.7	0.80 (0.72-0.87)

Table 3. Effects of the parameters for the diastolic and systolic phase for averaging over 3 phases and over 4 voxels.

	Single voxel			**4 central voxels**		
	Mean ± SD_{REP}	**CV (%)**	**ICC (95% CI)**	**Mean ± SD_{REP}**	**CV (%)**	**ICC (95% CI)**
VmaxM	37.1 ± 4.6	12.4	0.74 (0.64-0.82)	34.1 ± 4.0	11.7	0.75 (0.65-0.83)
DiamM	5.9 ± 0.39	6.6	0.88 (0.82-0.92)	6.0 ± 0.32	5.3	0.86 (0.80-0.91)
MWSS	1.22 ± 0.19	15.6	0.82 (0.74-0.88)	1.05 ± 0.15	14.3	0.84 (0.77-0.89)

Table 4. Effect of averaging over 4 central voxels for the parameters averaged over the cardiac cycle.

Averaging in time improved reproducibility without major effects on the results. The largest effects were on FlowS, VmaxS and SWSS which decreased 10.6%, 8.7% and 6.5% respectively. The averaging of Vmax over the four central voxels decreased VmaxM and WSSM by respectively 10% and 14% but the reproducibility increased. The method with averaging has successfully been used in several studies with patients (13,14). For studies with follow-ups or for double blind studies it is beneficial to use the averaging and calculate WSS4 instead of WSS. In a study with young and elderly volunteers we did show that we could measure the WSS decline with age but also that a paraboloid can not be used to subscribe all differences between young and elderly volunteers (22).
When the inertia forces become important in a pulsatile flow, the velocity profile starts to deviate from a paraboloid. When the Womersley number is large, the deviation from the parabolic velocity profile is substantial. The Womersley number is defined as α=R.sqrt(ω/ν), where R is the radius, ω is the frequency of the pulsation and ν is the kinematic viscosity (2,23). When a blood density of 10^3 kg.m^{-3}, a frequency of 1 Hz, and a diameter of 3 mm is assumed, $\alpha = 3.4$. If the pressure gradient is always positive there are only minor distortions from a parabolic velocity profile for this Womersley number. In the ICA 4 cm distal to the bifurcation there is a forward pressure gradient during the complete cardiac cycle, so that the velocity profile can assumed to be approximately parabolic.
A drawback of this study was that PPU-gating was used for the rescanning and repositioning measurements; whereas ECG-gating was used for assessment of the one week and one month follow-up measurements. This has been caused by unavailability of vector ECG at the time this study started. By using PPU-gating the peak systolic flow can be detected after peak flow has occurred in the carotid artery. We expect this to be the cause of the ratio FlowS/FlowD being 1.97 in the PPU-gated part and 2.43 in the ECG-gated part.
This study has proven that WSS analyses based on the paraboloid model can give reproducible results. Gnasso showed that WSS calculation by the paraboloid method has proven to correlate inversely to age, systolic blood pressure and body mass index (3). Modelling of the velocity profile by a paraboloid is most commonly applied for echo Doppler in the common carotid artery. Our MWSS shows very good agreement with echo-Doppler measurements that have been reported by others (3,10,11). The age of the healthy male subjects in the reproducibility study of Gnasso et al. was 35.9 ± 3.7 years and their MWSS is 1.27 Pa ± 0.22 Pa (3). Samijo et al. found a MWSS of 1.12 ± 0.18 Pa (females) to 1.39 ± 0.19 Pa (males) for the group between 20 and 29 years of age (24). The mean age in our group is 26.8 ± 6.0 years and the average MWSS is 1.22 ± 0.19 Pa. With spatial averaging the average MWSS4 is 1.05 ± 0.15 Pa. Thus our results are comparable with the results of Samijo et al. and Gnasso et al. Also our velocity measurements, which were averaged over the cardiac cycle, are in good agreement with previously published observations (3). However, the SWSS we observed was lower than what has been observed by others using ultrasound. This difference is mainly caused by the Vmax which in our hands had approximately half the value (54.1 cm/s) as reported previously by Gnasso et al. (97.1 cm/s) (3). The reason for this discrepancy is probably based on the fact that our peak systolic velocity is assessed during sampling over 1/16 of the cardiac cycle (6.25 % ≈ 62.5 ms). With Doppler ultrasound the time resolution is much higher and systolic velocity is measured during the parts of micro-seconds with the highest Vmax. The standard deviation of our WSS measurements is comparable to echo-Doppler.
WSS assessment with MRI is less commonly applied but Zhao measured WSS in the internal carotid by Phase-Contrast MRI. Zhao observed for healthy volunteers a MWSS of 1.9 Pa on average for an age group of 30 years and a MWSS of 1.4 Pa for an age group of

80 years. These values are somewhat higher than those we observed. However Zhao calculated WSS by the following formula:

$$WSS = 32\ \mu\ Q / \pi\ D^3 \qquad (5)$$

Due to the limited resolution, the diameter (D) is difficult to measure directly with MRI. With D to the third power in the denominator large standard deviations can be expected. Samijo measured the intrasubject intrasession variability with ultrasound (24). His CV is approximately the same as ours for the SWSS and MWSS. Glor measured the reproducibility caused by operator dependence of WSS assessment with the Finite Element Method. The error in WSS was 21%, which means that our method is superior in reproducibility (25). In another study Glor compared WSS calculations based on MRI and ultrasound (26). Both his and our results indicate that the WSS with echo-Doppler and with MRI are of similar precision. However Glor's method is not automated (26). Echo-Doppler has the advantage of a high temporal resolution, but MRI is able to assess also WSS in vessels deeper into the body (7,9). Both MRI and echo-Doppler are sensitive to angulation. For echo-Doppler the angle between the major flow direction and the transducer has to be between 44° and 56°. For MRI the measured cross section of the vessel has to be perpendicular to the major flow direction. A possible extension of this method for MRI is that MWSS can also be assessed for untriggered MR measurements.
In conclusion: The method proposed in this study permits rapid, semi-automatic WSS measurements in the internal carotid artery. With this method WSS measurements based on a standard MR acquisition technique can be incorporated in clinical MRI protocols. The advantages of this automatic method over manual methods are shorter analysis time, the absence of inter- and intra- observer variability and a better reproducibility.

Grant support

Financed by the Netherlands Heart Foundation Grant 2000.119

References

1. Malek AM, Alper SL, Izumo S. Hemodynamic Shear Stress and its Role in Atherosclerosis. *JAMA* 1999:282(21):2035-2042

2. Massey B, Ward-Smith J. Mechanics of fluids, United Kingdom: Stanley Thornes;1998:209

3. Gnasso A, Carallo C, Irace C et al. Association Between Intima-Media Thickness and Wall Shear Stress in Common Carotid Arteries in Healthy Male Subjects. *Circulation* 1996;94:3257-3262

4. Bakker CJG, Kouwenhoven M, Hartkamp MJ, Hoogeveen RM, Mali WPTM. Accuracy and precision of time-averaged flow as measured by nontriggered 2D phase-contrast MR angiography, a phantom evaluation. *MRI* 1995;13(7):959-965

5. Debatin JF, Ting RH, Wegmuller H et al. Renal-artery blood-flow-quantification with phase contrast MR-imaging with and without breath-holding. *Radiology* 1994;190(2):371-378

6. Nichols WH and O'Rourke MF. Blood flow in arteries. Edward Arnold 1998.

7. Silber HA, Bluemke DA, Ouyang P , Du YP, Post WS, Lima JAC. The relationship between vascular wall shear stress and flow mediated dilation: Endothelial function assessed by phase-contrast magnetic resonance angiography. *J Am Coll Cardiol* 2001;38(7):1859-1865

8. Jiang Y, Kohara K, Hiwada K. Low Wall Shear Stress contributes to atherosclerosis of the carotid artery in hypertensive patients. *Hypertension Res Clin Exp* 1999; 22(3):203-207

9. Zhao M, Charbel FT, Loth F et al. Wall Shear Stress in major arteries as function of age measured by cine Magnetic Resonance Imaging. In: Proceedings of the 8th annual meeting of ISMRM, Denver, 2000. (abstract 1653)

10. Carallo C, Irace C, Pujia A. Evaluation of common carotid hemodynamic forces-Relations with wall thickening. *Hypertension* 1999;34(2):217-221

11. Irace C, Carallo C, Cresenzo A et al. NIDDM is associated with lower wall shear stress of the common carotid artery. *Diabetes* 1999;48(1):193-197

12. Box FMA, Spilt A, Van Buchem MA, van der Geest RJ, Reiber JHC. Automatic model based contour detection and blood flow quantification in small vessels with velocity encoded MRI. *Invest Radiol* 2003;38(9):567-577

13. Ten Dam VH, Box FMA, de Craen AJM et al. Effect of pravastatin on cerebral blood flow and parenchyma volume in elderly at risk for vascular disease. *Stroke* 2005;36:1633-1636

14. Box FMA, Meinders IH, van der Geest RJ et al. The effect of Pravastatin on the Wall Shear Stress in the internal carotid artery; results from the PROSPER study', Proceedings ISMRM, Miami, (Florida) 2005

15. Spilt A, Box FMA, van der Geest R.J, Reiber JHC et al. Reproducibility of total cerebral blood flow measurements using phase contrast Magnetic Resonance Imaging. *JMRI* 2002;16(1):p1-5

16. Van der Geest RJ, Niezen RA, Van der Wall EE, de Roos A, Reiber JHC. Automatic measurements of volume flow in the ascending aorta Using MR velocity maps: Evaluation of inter- and intraobserver variability in healthy volunteers. *J Comput Assist Tomogr* 1998;22(6):904-911

17. Lotz J, Meier C, Leppert A, Galanski M. Cardiovascular flow measurement with phase-contrast MR Imaging: basic facts and implementation. *Radiographics* 22;2002:651-671

18. JHC Reiber, G Koning, GD Von Land, PMJ van der Zwet. In JHC Reiber and PW Serruys, editors. Why and how should QCA systems be validated? Progress in quantitative coronary arteriography. Dordrecht: Kluwer Academic Publishers; 1994. p 33-48

19. Fleiss JL. The design and analysis of clinical experiments. John Wiley & Sons 1986:8-1

20. Bland JM, Altman DG. Statistical methods for assigning agreement between two methods of clinical measurement. *Lancet* 1986;1:307-310

21. Saam T, Ferguson MS, Yarnykh et al. Quantitative Evaluation of Carotis Plaque composition by In Vivo MRI. *Arterioscler Thromb Vasc Biol* 2005;25:234-239

22. Box FMA, van der Geest RJ, van Osch MJP, van der Grond J, de Craen AJM, Blauw GJ, van Buchem MA, Reiber JHC. Differences in velocity profiles between young and elderly healthy volunteers affect wall shear stress assessment with the paraboloid method in the internal carotid artery; a study with velocity encoded MRI. Proc World Congress Biomech, Munchen, 2006

23. Nichols WW, O'Rourke MF. McDonalds Blood flow in arteries, 1998 Forth edition Arnold, London, 22

24. Samijo SK, Willigers JM, Brands PJ et al. Reproducibility of shear rate and shear stress assessment by means of ultrasound in the common carotid artery of young human males and females. *Ultrasound in Med & Biol* 1997;23(4):583

25. Glor FP, Ariff B, Hughes AD et al. Operator dependence of 3D Ultrasound-based computational fluid dynamics for the carotid bifurcation. *IEEE Trans Med Imaging* 2005;24(4):451-456

26. Glor FP, Ariff B, Hughes AD et al. Image-based carotid flow reconstruction: a comparison between MRI and ultrasound. *Physiol Meas* 2004;25(6):1495-1509